Derivation and validation of a sensitivity formula for knife-edge slit gamma camera: A theoretical and Monte Carlo simulation study

Original Article

Etesam Malekzadeh[1], Hossein Rajabi[1], Elisa Fiorina[2,3], Faraz Kalantari[4]

[1]Department of Medical Physics, Faculty of Medical Sciences, Tarbiat Modares University, Tehran, Iran
[2]National Institute of Nuclear Physics, Section of Torino, Torino, Italy
[3]Clinical Department, Fondazione CNAO, Pavia, Italy
[4]Department of Radiation Oncology, University of Arkansas for Medical Sciences, Little Rock, Arkansas, USA

(Received 21 January 2021, Revised 15 June 2021, Accepted 17 June 2021)

ABSTRACT

Introduction: Gamma cameras are proposed for online range verification and treatment monitoring in proton therapy. An Analytical formula was derived and validated for sensitivity of a slit collimator based on the photon fluence concept.

Methods: Fluence formulation was generalized for photons distribution function and solved for high-energy point sources. The effect of the collimator slit size and source off-axis position on the sensitivity of the collimator were included in the formula.

Results: The analytically calculated sensitivities of the slit collimator were in good agreement with Monte Carlo results according to the Bland-Altman agreement test and Pearson correlation (r =0.998) statistical analysis with $p < 0.05$. The mean relative error between calculated sensitivities with the derived formula and Monte Carlo was up to 0.8%. Moreover, we found that under certain conditions, the established formula is converted to the Anger equation for the pinhole collimator.

Conclusion: The analytical formula developed in this research can estimate the slit collimator sensitivity with an acceptable accuracy. The derived closed-form sensitivity formula can be applied in KE collimator design and optimization studies.

Key words: Mathematical modeling; Gamma camera; Monte Carlo

Iran J Nucl Med 2021;29(2):86-92
Published: July, 2021
http://irjnm.tums.ac.ir

Corresponding author: Etesam Malekzadeh, Department of Medical Physics, Faculty of Medical Sciences, Tarbiat Modares University, Tehran, Iran. E-mail: e.malekzadeh@modares.ac.ir

INTRODUCTION

Detection of prompt gamma photons using gamma cameras is one of the most promising techniques for online range verification and treatment monitoring in proton therapy [1-3]. Physical collimators are the main component of the gamma detection system that play an essential role in determining the sensitivity and resolution of the camera. Among them, slit camera has been proposed for proton range verification and tested in clinical practices [4, 5]. A slit gamma camera, consists of a knife-edge slit collimator and a pixelated detector that makes it useful for high sensitivity 1D imaging that is desired when the imaging suffers from low count statistics [2].

The availability of analytical resolution and sensitivity formulas for a collimator is very important for collimator design optimization, system simulation, and also image reconstruction algorithms that use the collimator response during forward/backward projection process for resolution recovery [6-8] . In the prompt gamma-imaging context, it has been postulated that on-axis resolution of slit camera can be calculated using pinhole and slit-slat (SS) collimator formulas [9, 10] that is in good agreement with Monte Carlo (MC) results [10]. The overall resolution formula R for a pinhole and a slit-slat collimator is well established and is given by

$$R = \left[R_g^2 + \frac{h^2}{f^2}R_i^2\right]^{\frac{1}{2}} \qquad (1)$$

$$\left[w^2\frac{(h+f)^2}{f^2} + \frac{h^2}{f^2}R_i^2\right]^{\frac{1}{2}}$$

Where w is the pinhole width, h is the source distance from aperture plane, f is the focal length of collimator which is defined as distance from aperture to detector plane, R_g is the geometric collimator resolution, and R_i is the intrinsic detector resolution.

In another study, modified pinhole collimator formulas were suggested to calculate the slit collimator sensitivity and resolution [11]. In this study, the method of finding the formula is not presented in detail. The dependence of the efficiency on the distance of the source from the collimator varies with the inverse of the distance, which is inconsistent with the geometrical efficiency of the pinhole collimator and further attempts are needed to investigate the inconsistency. Their proposed formula for the geometric resolution is as equation 1 that is given by pinhole resolution formula [12]. In addition, the suggested collimator sensitivity formula is given by

$$g = \frac{w_{eff}}{4\pi h} \qquad (2)$$

Where w_{eff} is the effective slit width of the knife-edge collimator according to Metzler et al. [13].

Zhang et al. recently developed an analytical formula describing the collimator-detector response of the slit camera, but the system resolution and sensitivity were not considered in their model [14].

To the best of our knowledge, so far no theoretical basis has been provided for extracting the geometrical sensitivity of the knife-edge slit collimator. In this study we propose analytical models for a slit gamma camera that predicts geometrical sensitivity based on the geometrical parameters of the collimator and source position. To do this, we assumed that the sensitivity of a slit camera can be determined from the photons fluence function. The off-axis geometrical sensitivity of the collimator was modeled using the Accorsi et al. Formula [15]. Moreover, photon penetration through the collimator slit was considered based on the models presented by Accorsi et al. [15]. Analytical expression for the on-axis sensitivity of a slit camera are derived and validated by comparison to Monte Carlo (MC) simulation. The results were also compared with previously published data [11, 12, 16, 17].

METHODS

KE collimator reference setup

The schematic diagram of a slit collimator and pixelated detector variables is shown in Figure 1.

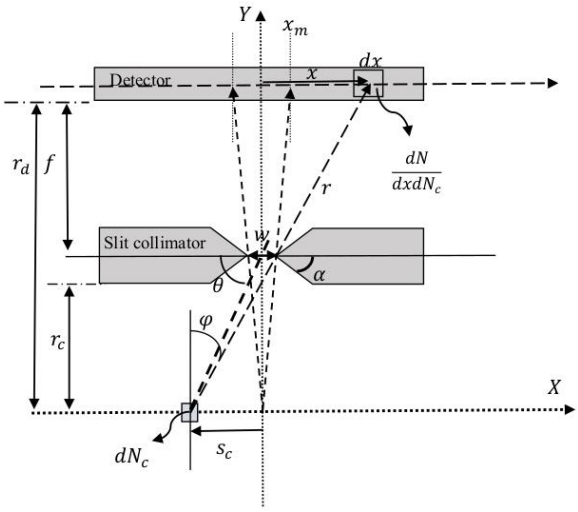

Fig 1. Geometric description of physical parameters for the KE collimator and pixelated detector.

The geometric parameters of the detection system, used in this study, are listed in Table 1. With reference to Figure 1, the z-axis (perpendicular to the plane) lies along the centerline of the slit, which has physical width of w'. The x-axis is also in the plane of the slit,

which has physical width of w. The source position is located at $(x = -s_c, y = 0, z = 0)$.

Table 1: Summary of the collimator and detector parameters.

Description	Parameter
Displacement angle	θ
Source position	s_c
Detector profile axis	x
Fluence angle	φ
Collimator slit angle	α
Source-to-detector distance	r_d
Source-to-collimator distance	r_c
Slit width	w
Crystal length	L
Focal length	f

Parameters of the collimator were selected similar to those of Smeets et al. [10] (Table 2). All calculations were performed for an isotropic point source with an energy of 4.4 MeV and a total of 10^8 emitted particles for MC simulation [18]. Tungsten linear attenuation coefficient is $\mu = 0.078mm^{-1}$ for this energy.

Table 2: Selected parameters for the camera.

Parameter	Value
Slit angle	63.4 degree
Slit width	6.0 mm
Source-to-collimator distance	150.0 mm
Crystal length	200.0 mm

Mathematical derivation of photon distribution function

The fluence of isotropically emitted photons from a point source of unitary activity, can be calculated using the following concept [19]:

The fluence of photons = (Effect of the inverse square of the distance) × (Effect of the non-perpendicular incidence of the photons on the detector plane)

$$\frac{1}{r^2} \times cos(\varphi) \qquad (3)$$

Where r is the source to the detector element distance, and φ is the angle between the line connecting the source point to point x on the detector plane and detector normal vector (Figure 1). The general expression of the photon distribution on the detector axis was derived from equation 1 followed the procedures outlined by Formiconi with following modifications [19]:

1) The aperture function of the collimator-detector system is initially not considered.
2) The distribution of detected photons is calculated only in the x-direction.
3) The differential source element was replaced with a point source.

Consequently, the distribution of detected photons is thus given by the following formula:

$$\frac{dN}{dxdN_c} = \frac{Lr_d}{4\pi\left((x-s_c)^2+r_d^2\right)^{\frac{3}{2}}} \qquad (4)$$

Where s_c is the source displacement and r_d is the detector distance (i.e., the source distance from the detector front plane).

In equation 4, $\frac{dN}{dxdN_c}$ indicates the number of photons recorded in the differential element per emitted photon. The collimator response was used to define the range of the integration interval in the calculation of the sensitivity such that the width of the collimator limits the number of active photon receptor crystals in the detector.

Derivation of the system on-axis sensitivity

Geometrical sensitivity of the collimator, is define as the fraction of photons emitted by a point source that passes through the collimator slit. In an attempt to derive the on-axis (i.e., $\left(s_c = 0, \theta = \frac{\pi}{2}\right)$) sensitivity, the integral of the equation 4 was calculated as:

$$g = \int_{-x_m}^{x_m} \left(\frac{dN}{dxdN_c}\right) dxdN_c \qquad (5)$$

$$= \int_{-w\frac{r_d}{2r_c}}^{w\frac{r_d}{2r_c}} \frac{Lr_d}{4\pi((x)^2 + r_d^2)^{\frac{3}{2}}} dx$$

$$\frac{wL}{4\pi r_d r_c} \times \frac{1}{\left(1 + \left(\frac{w}{2r_c}\right)^2\right)^{\frac{1}{2}}}$$

Moreover, to consider the effect of source displacement on the sensitivity, according to Accorsi et al., equation 5 was multiplied to$sin^3(\theta)$, where θ is the angle formed by the line drawn from a source (in the XY plane) to the center of the slit and the plane of the slit (the YZ plane) [15].

The effect of penetration through the slit material on the sensitivity was considered by the following formula [14]:

$$w_{eff} = w + \frac{0.693}{\mu tan(\alpha)} \qquad (6)$$

Referring to Figure 1 where w is the physical slit width, w_{eff} is the effective slit width considering the penetration , α is the slit angle and μ is the collimator attenuation coefficient factor, which was assumed that the collimator is made of Tungsten ($\mu = 0.078 mm^{-1}$for 4.4 MeV).

Taking into consideration that $\frac{L}{r_d} = \frac{w'}{r_c}$ based on the trigonometric relation where w' is the slit width along z axis. We can write the equation 5 as:

$$g = \frac{w'w}{4\pi r_c^2} \times \frac{1}{\left(1 + \left(\frac{w}{2r_c}\right)^2\right)^{\frac{1}{2}}} \qquad (7)$$

For pinhole collimator we have $w' = w$. In addition, source-to-collimator distance is much more than slit width for the most relevant imaging situations that $\frac{w}{2r_c} \ll 1$ and therefore, $\left(1 + \left(\frac{w}{2r_c}\right)^2\right)^{\frac{1}{2}} \approx 1$. Consequently, equation 7 can be simplified to:

$$g = \frac{w^2}{4\pi r_c^2} \qquad (8)$$

Equation 8 is the derived formula by Anger for pinhole collimator [11].

Monte Carlo simulation

Monte Carlo simulations were performed with GATE/GEANT4 code version 8.2. GATE is an open-source MC code for simulation of emission tomography and radiation therapy [20, 21]. This version of GATE is based on GEANT4 version 10.5.1. The Opt3 electromagnetic standard package called emOpt3 was used to simulate the photon interactions. To score the observables, fluence calculations were performed using "FluenceActor". The Qt software was also used for visualization of the geometry (Figure 2). The Origin software was used for data analysis. Bland-Altman agreement test and Pearson correlation statistical analysis with $p < 0.05$ were performed. The analytically derived values of the sensitivity and resolution for the slit collimator were compared to MC results, which is well known as the gold standard in particle transport calculations.

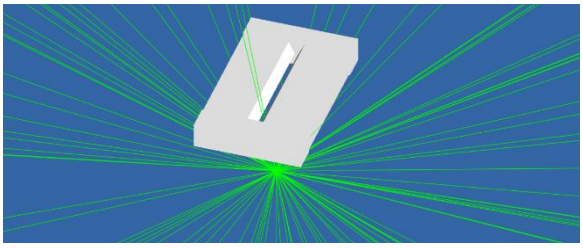

Fig 2. The geometry of the KE collimator with an isotropic point source.

RESULTS

Figure 3 shows the geometrical sensitivities according to the source-to-collimator aperture distance. Source-to-collimator distances are changing from 30 to 270 mm. The calculated sensitivities were within the range $3.2 \times 10^{-2} - 1.1 \times 10^{-3}$. To validate the derived formula, a comparison to previously proposed models were made. Furthermore, MC simulation results were also used to verify the derived model. "MC simple" indicates that the penetration and scattering effect were not considered in this step. According to our findings, the sensitivity changes with the source-to-collimator distance as r_c^{-2}. Correlation coefficient was calculated $r = 0.998$ for derived formula and MC simulation results. It shows that the results are highly correlated.

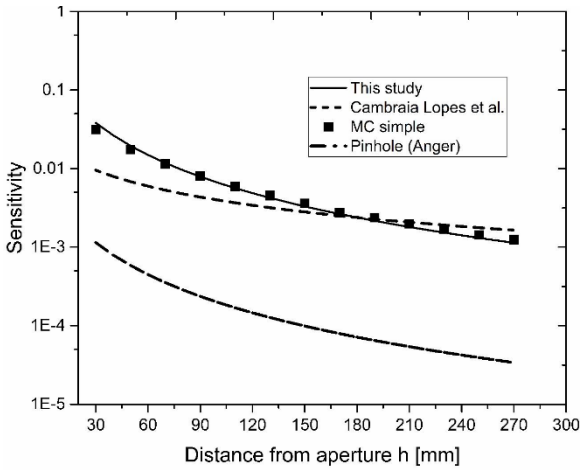

Fig 3. The variation of the collimator sensitivity versus source to collimator distance for pinhole, Monte Carlo, published data and the results of KE collimator.

Output of the Bland-Altman test for extracted results is reported in Figure 4. 10% limit of acceptance was selected for agreement test. Mean of differences is -0.8% and upper as well as lower limits are +9.2% and -10.8%, respectively.

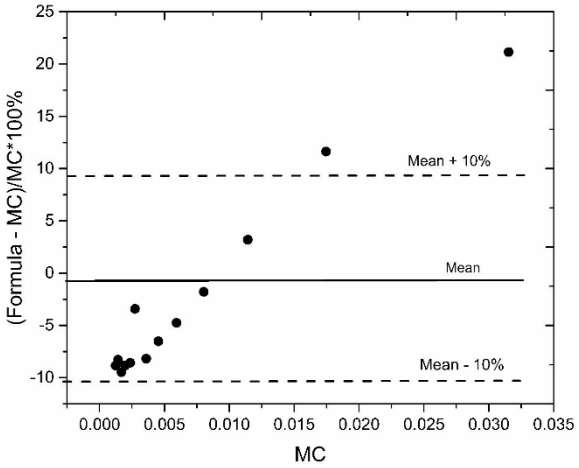

Fig 4. Bland-Altman agreement test of the formula and MC results is shown. The results do not include the penetration and scattering effect. Mean, upper and lower limits were illustrated in figure. The Limit of agreement (LOA) was set at 10%.

Sensitivity values against the source-to-collimator distance with taking into account the penetration effect were illustrated in Figure 5.

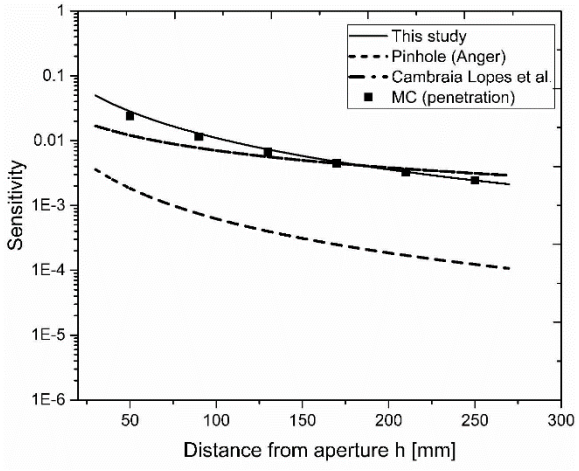

Fig 5. Sensitivity versus source-to-collimator distance when penetration effect was considered.

For the reference setup (Table 2), the calculated sensitivities were within the range $5.6 \times 10^{-2} - 2.1 \times 10^{-3}$, which is about two times more than the ideal case without including the penetration. In addition, according to Figure 5, there is an obvious discrepancy between the amount of sensitivity obtained with Pinhole formula, MC simulation and developed formula. Correlation coefficient was calculated $r = 0.999$ for collimator sensitivity derived from analytical formula and MC simulation results.

Off-axis sensitivities were calculated and compared to MC results (Figure 6). The source was moved in steps of 1.0 cm from the on-axis position to a distance of 8.0 cm. It was observed that at far distances from the on-axis position, the sensitivity decreases due to the effect of the thickness of the collimator wall (Figure 1 and 2). Correlation coefficient of $r = 0.984$ was calculated between analytical versus MC results.

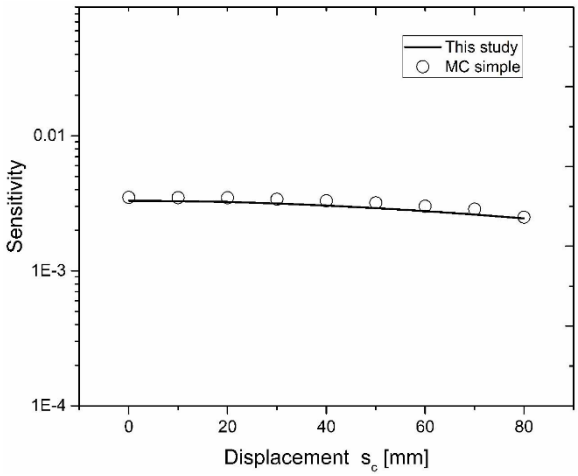

Fig 6. Angular dependency of the off-axis sensitivity.

DISCUSSION

In this study, the analytical formula to estimate the sensitivity based on the fluence distribution for slit collimator was derived and validated. We generalized Formiconi's formulation and solved it for high-energy photons emitted from point source [19]. The effect of penetration and attenuation of photons through the collimator slit were explicitly considered on geometrical sensitivity using validated models derived by Accorsi et al. [15]. Furthermore, the off-axis sensitivity was taken into account in the formula.

The aim of this study was to develop an analytical formula for the geometrical sensitivity of slit collimator. However, photons penetration through the knife-edge slit was considered, but also scattering affects the sensitivity. The scattering effect was not considered in our study. Also, the high background radiation that mainly originates from neutrons were not considered in this study. However, ignoring this case does not affect the geometrical sensitivity of the collimator.

It was found that, for source-to-collimator distances above 180 mm, the proposed model by Lopes et al. overestimates the sensitivity up to 31.0% [11]. The sensitivity for the pinhole collimator was plotted against the source-to-collimator distance and is shown in Figure 3. Using the pinhole sensitivity formula, it is observed that the sensitivity of the collimator is about 10 times lower compared to the Monte Carlo results.

Our results showed that the calculated sensitivities are in good agreement with the MC results. We found that the slit collimator has a distance dependence of r_c^{-2} for its on-axis sensitivity. This is consistent with MC simulation. On the other hand, this finding is

inconsistent with the developed formula by Lopes et al. which predicts distance dependence asr_c^{-1} [11]. However, according to the obtained formula for KE camera, for a fixed source-to-detector distance, derived formula can estimate the r_c^{-1}dependency. Furthermore, we explained that in certain conditions, the derived sensitivity can predict the pinhole collimator sensitivity, which is derived by Anger. So, in comparison with pinhole collimator, the efficiency of the knife edge collimator can be written as follows:

$$g = kw'w/4\pi h^2 \qquad (9)$$

Here, w' is the transverse width of the collimator and k is a coefficient that is equal to 1 for the pinhole collimator. With this postulation, the sensitivity changes with distance as the inverse square, which does not agree with the formula developed by Cambria Lopes et al. [11].

The derived analytical formula indicated that the sensitivity of the slit collimator varies linearly with the width of the slit (equation 7). Therefore, the slit width dependence of sensitivity is consistent with the slit-slat collimator's [13] and is inconsistent with the pinhole collimator's, where the sensitivity is proportional to the square of the slit width. Also, our findings is in agreement with Lopes et al.' results that showed the linear variation of the sensitivity with the slit width in slit collimators. A possible explanation for this might be the one dimensional collimating feature of the slit collimator. Another study has been conducted to design the U-SPECT-II imaging system using a multi-pinhole collimator for ultra-high resolution small animal imaging. In their study, the geometric sensitivity was reported at 0.07% and 0.18% for the collimator with 0.35- and 0.6-mm pinholes, respectively. This result represents that sensitivity of the U-SPECT-II is proportional to the square of the pinhole aperture width [17].

To consider the penetration through the collimator slit, Lopes et al. [11] used the equation for the pinhole collimator derived by Metzler et al. [13], whereas we used the developed formula by Accorsi et al. [15] for the slit-slat collimators. The current study showed that the penetration effect is a highly significant component. By comparing the slit width with and without considering the penetration effect, for instance, one finds for 4.4 MeV and tungsten an effective slit width w_{effe}= 10.5 mm for a physical slit width w = 6.0 mm. Furthermore, comparison of our results with MC simulation confirmed that the effective slit formulas derived by Accorsi et al. [15] are valid for high-energy photons.

Different geometries have been designed for pinhole collimators such as knife-edge and lofthole shape geometries [16]. They reported the sensitivity dependency to source-to-collimator distance as an inverse square that is in agreement with our derived formula. However, the circular aperture shape leads to different amounts of sensitivity. Also, penetration effect did not take into account for lofthole collimator. In addition, slit collimators are useful for high energy prompt gamma detection in radiation therapy applications, whereas lofthole collimator has been designed for radionuclide imaging purposes in nuclear medicine.

Accorsi et al. showed that the slit-slat collimator has $sin^3(\theta)$ sensitivity dependence [15]. Moreover, Monte Carlo and experimental studies have shown that the slit-slat collimator has $sin^a(\theta)$sensitivity dependence where a is greater than three. In this study, we applied this dependency to take into account the source displacement s_c effect on the sensitivity of the slit collimator. By comparing our results with MC, it is clear that our findings further support $sin^a(\theta)$sensitivity dependence of the slit collimator. Further work is required to establish an exact value for$a$.

The closed-form sensitivity formula can be applied in collimator design studies across MC simulations. Therefore, the importance of our proposed formula thus lies both in its speed and its relative ease of application in slit collimator design and optimization studies.

CONCLUSION

The analytical formula developed in this research can estimate the slit collimator sensitivity with an acceptable accuracy. Due to the promising results of gamma cameras with knife edge collimators, another type of imaging system may be designed based on this collimator. To do this, analytical formulas alongside Monte Carlo methods can be used in the design and optimization stages. The sensitivity formula also provides distance dependency that agrees well with the Monte Carlo simulation results. The formula is useful for designing new slit cameras based on the slit collimator geometry. This closed-form expression may be also incorporated into model-based reconstruction algorithms in an efficient manner. Finally, the formula can help to better understand the consequences of the collimator design choices.

Acknowledgements

This work received a grant according to the code (ID: 76401) for the Ph. D. thesis from the Faculty of Medical Sciences, Tarbiat Modares University.

REFERENCES

1. Krimmer J, Dauvergne D, Létang J, Testa É. Prompt-gamma monitoring in hadrontherapy: A review. Nucl

Instrum Methods Phys Res A: Accel Spectrom Detect Assoc Equip. 2018;878:58-73.

2. Parodi K. Latest developments in in-vivo imaging for proton therapy. Br J Radiol. 2020 Mar;93(1107):20190787.

3. Fischetti M, Baroni G, Battistoni G, Bisogni G, Cerello P, Ciocca M. Inter-fractional monitoring of [Formula: see text]C ions treatments: results from a clinical trial at the CNAO facility. Sci Rep. 2020 Nov 26;10(1):20735.

4. Richter C, Pausch G, Barczyk S, Priegnitz M, Keitz I, Thiele J, Smeets J, Stappen FV, Bombelli L, Fiorini C, Hotoiu L, Perali I, Prieels D, Enghardt W, Baumann M. First clinical application of a prompt gamma based in vivo proton range verification system. Radiother Oncol. 2016 Feb;118(2):232-7.

5. Xie Y, Bentefour EH, Janssens G, Smeets J, Vander Stappen F, Hotoiu L, Yin L, Dolney D, Avery S, O'Grady F, Prieels D, McDonough J, Solberg TD, Lustig RA, Lin A, Teo BK. Prompt gamma imaging for in vivo range verification of pencil beam scanning proton therapy. Int J Radiat Oncol Biol Phys. 2017 Sep 1;99(1):210-218.

6. Kalantari F, Rajabi H, Saghari M. Quantification and reduction of the collimator-detector response effect in SPECT by applying a system model during iterative image reconstruction: a simulation study. Nucl Med Commun. 2012 Mar;33(3):228-38.

7. Mahani H, Raisali G, Kamali-Asl A, Ay MR. Collimator-detector response compensation in molecular SPECT reconstruction using STIR framework. Iran J Nucl Med. 2017;25(Suppl 1):26-34

8. Metzler SD, Bowsher JE, Smith MF, Jaszczak RJ. Analytic determination of pinhole collimator sensitivity with penetration. IEEE Trans Med Imaging. 2001 Aug;20(8):730-41.

9. Bom V, Joulaeizadeh L, Beekman F. Real-time prompt gamma monitoring in spot-scanning proton therapy using imaging through a knife-edge-shaped slit. Phys Med Biol. 2012 Jan 21;57(2):297-308

10. Smeets J, Roellinghoff F, Prieels D, Stichelbaut F, Benilov A, Fiorini C. Prompt gamma imaging with a slit camera for real-time range control in proton therapy. Phys Medicine Biol. 2012 Jun 7;57(11):3371-405.

11. Lopes PC, Pinto M, Simões H, Biegun A, Dendooven P, Oxley D, Parodi K, Schaart DR, Crespo P. Optimization of collimator designs for real-time proton range verification by measuring prompt gamma rays. 2012 IEEE Nuclear Science Symposium and Medical Imaging Conference Record (NSS/MIC); 2012.

12. Anger HO. Radioisotope cameras. In: Hine GJ. Instrumentation in Nuclear Medicine. London: Academic Press; 1974.

13. Metzler SD, Accorsi R, Novak JR, Ayan AS, Jaszczak RJ. On-axis sensitivity and resolution of a slit-slat collimator. J Nucl Med. 2006 Nov;47(11):1884-90.

14. Zhang D, Fan P, Lu W, Wang S, Xia Y, Wu Z, et al., editors. Accurate Modeling of Multi Knife-edge Slit Collimator System Response for MeV Prompt Gamma Photons in Proton Therapy Monitoring. 2018 IEEE Nuclear Science Symposium and Medical Imaging Conference Record (NSS/MIC); 2018.

15. Accorsi R, Novak JR, Ayan AS, Metzler SD. Derivation and validation of a sensitivity formula for slit-slat collimation. IEEE Trans Med Imaging. 2008 May;27(5):709-22.

16. Deprez K, Pato LR, Vandenberghe S, Van Holen R. Characterization of a SPECT pinhole collimator for optimal detector usage (the lofthole). Phys Med Biol. 2013 Feb 21;58(4):859-85.

17. Van Der Have F, Vastenhouw B, Ramakers RM, Branderhorst W, Krah JO, Ji C. U-SPECT-II: an ultra-high-resolution device for molecular small-animal imaging. J Nucl Med. 2009 Apr;50(4):599-605.

18. Hilaire E, Sarrut D, Peyrin F, Maxim V. Proton therapy monitoring by Compton imaging: influence of the large energy spectrum of the prompt-γ radiation. Phys Med Biol. 2016 Apr 21;61(8):3127-46.

19. Formiconi AR. Geometrical response of multihole collimators. Phys Med Biol. 1998;43(11):3359.

20. Jan S, Benoit D, Becheva E, Carlier T, Cassol F, Descourt P. GATE V6: a major enhancement of the GATE simulation platform enabling modelling of CT and radiotherapy. Phys Med Biol. 2011;56(4):881.

21. Strulab D, Santin G, Lazaro D, Breton V, Morel C. GATE (Geant4 Application for Tomographic Emission): a PET/SPECT general-purpose simulation platform. Nucl Phys B-Proc Suppl. 2003;125:75-9.